The upgrade of the ATLAS first-level calorimeter trigger

Shimpei Yamamoto[a], on behalf of the ATLAS Collaboration

[a] *International Center for Elementary Particle Physics, the University of Tokyo, Tokyo, Japan*

Abstract

The first-level calorimeter trigger (L1Calo) had operated successfully through the first data taking phase of the ATLAS experiment at the CERN Large Hadron Collider. Towards forthcoming LHC runs, a series of upgrades is planned for L1Calo to face new challenges posed by the upcoming increases of the beam energy and the luminosity. This article reviews the ATLAS L1Calo trigger upgrade project that introduces new architectures for the liquid-argon calorimeter trigger readout and the L1Calo trigger processing system.

Keywords: Calorimeters, Data acquisition, Electronic circuits
PACS: 07.20.Fw, 07.05.Hd, 84.30.-r

1. Introduction

The increases of beam energy and luminosity of the Large Hadron Collider (LHC) in the coming years open a faster way to physics goals of the ATLAS experiment [1]. However, the hardware-based first-level calorimeter trigger (L1Calo) is required to cope with challenges as:

– Degradations and baseline shifts of the signals due to the signal length and severe pile-up levels.

– High L1Calo trigger rates induced by the large number of jets originating from pp collisions in each bunch crossing.

As summarized in Table 1, in the data taking period foreseen in 2019–2022 (Run-3), the LHC is expected to operate at a luminosity well beyond the design value of 10^{34} cm^{-2}s^{-1}. The present trigger system therefore has to be upgraded to deal with these difficulties and preserve the physics acceptance by replacing the Run-1 hardware with improved trigger and readout electronics

This article reviews the upgrade project of the ATLAS L1Calo trigger system for the Run-3 data taking, referred to as phase-1 upgrade: it involves two new architectures for the trigger readout of the liquid-argon (LAr) calorimeters and the L1Calo trigger processing system [2, 3] to make use of higher granularity and run better performing trigger algorithms. The system for the data taking in 2015–2017 (Run-2) is also described.

2. ATLAS calorimeter and trigger system

The ATLAS calorimeter system covers a pseudo-rapidity range of $|\eta| < 4.9$ [1]. The electromagnetic (EM) calorimeter is a lead/LAr detector in the barrel ($|\eta| < 1.475$) and endcap ($1.375 < |\eta| < 3.2$) regions. The hadron calorimeters are composed of a steel and scintillator-tile barrel ($|\eta| < 1.7$), a LAr/copper endcap ($1.5 < |\eta| < 3.2$) and a LAr forward system ($3.1 < |\eta| < 4.9$) with copper and tungsten absorbers.

Table 1: Collision energy, instantaneous luminosity ($\mathcal{L}$) and the mean number of collisions per bunch crossing ($< \mu >$) for Run-1 and forthcoming data taking periods.

Period	$\sqrt{s}$ [TeV]	$\mathcal{L}$ [cm^{-2}s^{-1}]	$< \mu >$
2009–2013 (Run-1)	7–8	$\sim 0.8 \times 10^{34}$	~ 20
2015–2017 (Run-2)	13–14	$\sim 1.6 \times 10^{34}$	~ 40
2019–2022 (Run-3)	14	$\sim 3.0 \times 10^{34}$	~ 80

The L1Calo system processes signals from the EM and hadronic calorimeters in a pipeline and provides trigger signals to the Central Trigger Processor (CTP). The inputs to the L1Calo system are so-called Trigger Towers that are formed by analog summation of calorimeter cells across the longitudinal layers in a region of $\Delta\eta \times \Delta\phi = 0.1 \times 0.1$. These signals are sampled in the Pre-Processor Modules (PPMs) at a frequency of 40 MHz [2] and processed to provide calibrated transverse energy (E_{T}) time-aligned to the correct bunch crossing (bunch-crossing identification). The resultant digital data are transmitted to the Cluster Processor and Jet-Energy Processor subsystems in which e/γ candidate, τ and jet are identified, respectively. The Jet-Energy Processor also provides the total E_{T} and the magnitude of missing transverse momentum ($E_{\mathrm{T}}^{\mathrm{miss}}$). Trigger multiplicity information is then sent to the CTP via Common Merger Modules (CMMs).

Email address: shimpei.yamamoto@cern.ch (Shimpei Yamamoto)

[1] ATLAS uses a right-handed coordinate system with its origin at the nominal interaction point (IP) in the center of the detector and the z-axis coinciding with the axis of the beam pipe. The x-axis points from the IP to the center of the LHC ring, and the y-axis points upward. Cylindrical coordinates (r, ϕ) are used in the transverse plane, ϕ being the azimuthal angle around the beam pipe. Pseudorapidity is defined in terms of the polar angle θ as $\eta = -\ln\tan(\theta/2)$.

[2] Corresponding to the LHC bunch-crossing rate.

2.1. *Improvements toward forthcoming LHC runs*

The Trigger Towers used in the present L1Calo system are too coarse and the extraction of object features such as e, γ, τ and jets is challenging at high luminosities. High pile-up levels degrade the calorimeter resolution and compromise isolation requirements for particles, thereby degrading the trigger performance. A primary handle in high-luminosity conditions is therefore to make use of increased granularity for the trigger processing similar to off-line software algorithms. Figure 1 shows the distributions of variables representing lateral shower shape and longitudinal shower leakage: these are calculated with higher granularity for jets and electrons from Z decays. This shower-shape information is of use to discriminate EM showers from jets.

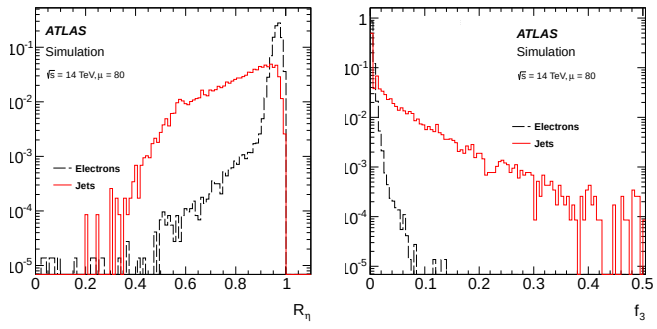

(a) Lateral shower shape (b) Longitudinal shower leakage

Figure 1: Distributions of R_η (a) and f_3 (b) variables representing lateral shower shape and longitudinal shower leakage. Definitions of these variables are given in Ref. [2]. Samples used are produced using a detector simulation described in Ref. [4].

3. Upgraded trigger readout of the LAr calorimeters

Following the strategy described above, a new readout element as the input to the L1Calo algorithms, referred to as Super Cell, is employed to achieve a new trigger readout scheme with higher granularity. It provides information for each calorimeter layer as well as finer segmentation: in the central calorimeter region, ten Super Cells correspond to a Trigger Tower. Detailed descriptions of the Super Cells are given in Fig. 2 and Table 2.

Table 2: η- and ϕ-granularities of the Trigger Tower and the Super Cell in the LAr barrel calorimeter.

	LAr barrel layers			
	Presampler	Front	Middle	Back
	$(\Delta\eta \times \Delta\phi)$			
Elementary cell	0.025×0.1	0.003125×0.1	0.025×0.025	0.05×0.025
Trigger Tower	0.1×0.1			
Super Cell	0.1×0.1	0.025×0.1	0.025×1	0.1×0.1

For the processing of signals from the Super Cells, LAr Trigger Digitizer Boards (LTDBs) and LAr Digital Processing

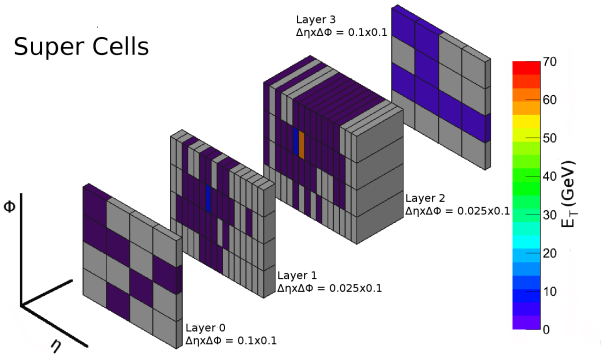

Figure 2: Geometrical representation of the Super Cells with the energy depositions of a simulated electron shower.

Blades (LDPBs) are newly introduced. The LTDBs are installed in the on-detector front-end crates with a replacement of the layer sum boards for the front and middle layers. The ADCs on the LTDB are custom ASICs: they have a 12-bit dynamic range and digitize the Super Cell signal at a frequency of 40 MHz with low power consumption ($<$ 50 mW per channel). Each board processes up to 320 Super Cells and sends serialized ADC sampling data to LDPBs using 5.12 Gbps optical links.

The LDPB consists of an ATCA-standard carrier blade equipped with four Advanced Mezzanine Cards (AMCs). The AMC is made around a powerful FPGA and high-speed optical transceivers: it receives the ADC sampling data from a LDPB and coverts them to calibrated E_{T} with the bunch-crossing identification by adopting digital filtering techniques, and finally transmits the data to the L1Calo system. In total 31 LDPBs are installed in three ATCA shelves. The resulting rates of receiving and transmitting data are $\sim$ 25 Tbps and $\sim$ 41 Tbps, respectively.

Figure 3 (a) and (b) illustrate a schematic view of the LTDB and the LDPB. A demonstrator system using LTDB and LDPB prototypes has been integrated in the Run-2 data taking, which enables us to validate the new trigger readout chain and perform an in-situ test of the digital filtering algorithms on collision data.

3.1. *Energy reconstruction of the Super Cell signal*

The LAr ionization signal has a triangular shape and a length given by the drift time of 450–600 ns in the barrel layer. It is bipolar-shaped with a time constant of 13 ns, resulting in a fastly rising but long signal shape compared to the LHC bunch spacing of 25 ns. Therefore, as the luminosity increases, the signal pulse shape is distorted due to an overlap with out-of-time pile-up pulses. The important features of the LDPB are a correction of out-of-time pile-up and a correct bunch-crossing identification in high pile-up conditions by digital filtering techniques over consecutive ADC sampling data. An example application by adopting a Wiener filter is shown in Fig. 4. By applying an active out-of-time pile-up correction, it achieves the ability to identify pile-up pulses overlapping in time, which gives a robust performance on the energy reconstruction and the bunch-crossing identification in high pile-up conditions.

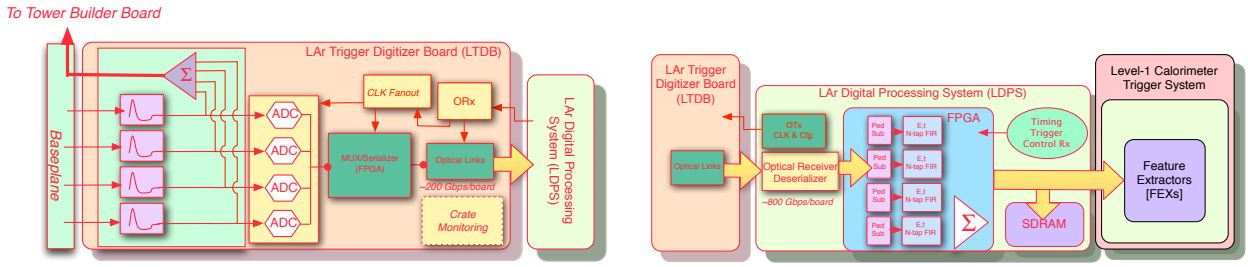

(a) LTDB (b) LDPB

Figure 3: Schematic view of the LAr trigger digitizer board LTDB (a) and the LAr digital processing blade LDPB (b).

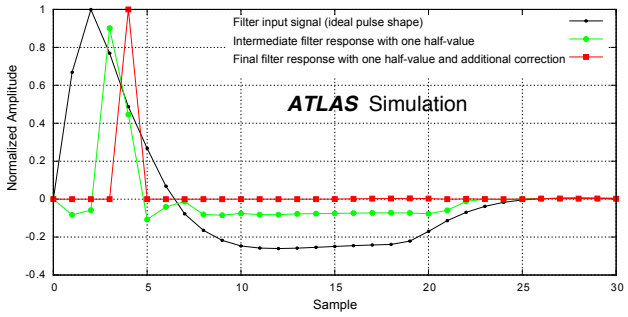

Figure 4: Illustration of the Wiener filter running on a Super Cell signal [2]. The Super Cell signal sampled at each bunch crossing is indicated by filled circles in black. Intermediate and final outputs of the filter are shown by filled circles in green and red, respectively. An single peak of the final output is observed after a given latency for processing, and its height corresponds to the energy.

4. Upgraded architecture of the calorimeter trigger processing system

Prior to the phase-1 upgrade in which more refined processing is possible with the new LAr trigger readout architecture, a number of upgrades were made in the L1Calo system to control trigger rates in Run-2. The PPM adopts a new Multi-Chip Module, which provides 80 MHz digitization and more flexible signal processing with a FPGA, in particular for handling of pile-up subtraction. The CMMs which manage the signals from the individual Processor boards are exchanged with newly designed ones (so-called CMX boards) to enable the data transmission to L1Topo. The L1Topo processes real-time event information based on the geometrical and kinematic relations between trigger objects, therefore, it is capable of forming combined trigger objects, as well as event-level quantities such as $E_{\mathrm{T}}^{\mathrm{miss}}$ and invariant mass. The L1Topo consists of two ATCA-standard blades equipped with two processing FPGAs each.

In the phase-1 upgrade, following the integration of the new LAr trigger readout architecture, the L1Calo system introduces new ATCA-standard modules that process high-granularity calorimeter information provided by the Super Cells and the tile barrel calorimeter data digitized in the PPMs, to extract object identification features. A schematic view of the upgraded L1Calo architecture for Run-3 is shown in Fig. 5. The L1Calo system employs three types of feature extractor modules dedicated for e/γ, jet and large-area jet, referred to as eFEX, jFEX and gFEX, respectively. These modules have similar architectures but run identification algorithms using different algorithm window sizes and granularities, depending on the targeted object features. The resulting number of modules for eFEX, jFEX, and gFEX is 24, 8, and 2, respectively. Table 3 summarizes the baseline system parameters and functionalities of the feature extractor modules.

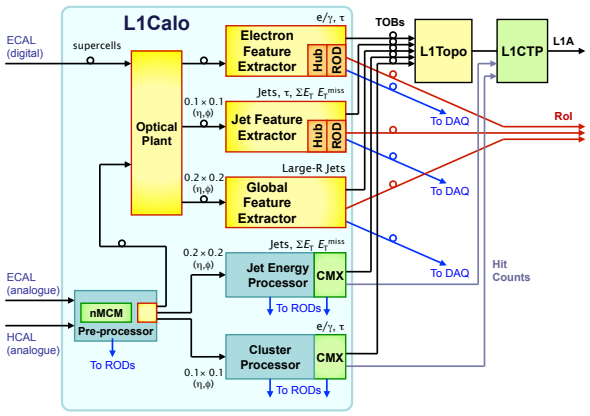

Figure 5: Schematic view of the upgraded L1Calo system architecture for Run-3.

Table 3: System parameters and functionalities of the feature extractor modules.

	Window ($\Delta\eta \times \Delta\phi$)	Granularity ($\Delta\eta \times \Delta\phi$)	Functionality
eFEX	0.3×0.3	Super Cell	Shower-shape variables, flexible rejection algorithms.
jFEX	0.9×0.9	0.1×0.1	Pile-up suppression using event energy density, flexible jet algorithms.
gFEX	1.8×1.8	0.2×0.2	Large-area jets e.g. for tagging boosted bosons.

5. Expected performance with the upgraded calorimeter trigger system

Improved resolution of the upgraded L1Calo results in better trigger efficiencies and more manageable rates. Selected examples of these improvements are described below.

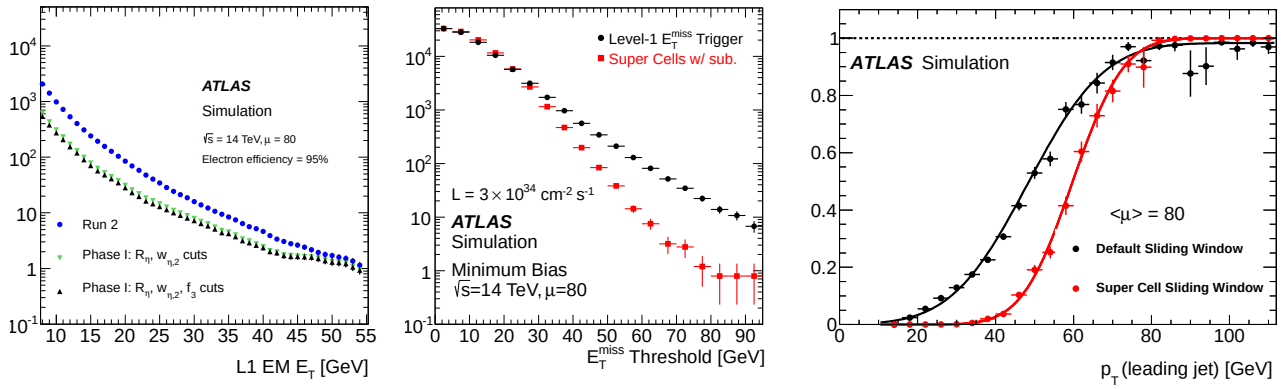

(a) EM-object trigger rates (b) $E_{\mathrm{T}}^{\mathrm{miss}}$ trigger rates (c) Trigger efficiency for jets

Figure 6: L1 trigger rates and efficiencies for electrons (a), $E_{\mathrm{T}}^{\mathrm{miss}}$ (b) and jets (c) [2]. The expectations with and without application of the shower-shape information are shown.

5.1. Single-object triggers

Figure 6 shows the first-level (L1) trigger rates for electrons and $E_{\mathrm{T}}^{\mathrm{miss}}$, and the efficiency for jets as a function of given E_{T} threshold. The feasibility of using low thresholds is important for the physics program and detector calibration. Thanks to the implementation of the shower-shape variables, maintaining a 95% trigger efficiency for electrons, the EM trigger threshold can be lowered from 28.5 GeV to 21.5 GeV for a given bandwidth of 20 kHz. The pile-up suppression and dedicated jet selection algorithms also reduce the $E_{\mathrm{T}}^{\mathrm{miss}}$ trigger rate and improve the trigger turn-on for jets.

5.2. Topological triggers

One prominent feature achieved by the upgraded calorimeter trigger system is the capability to run triggers using topological information in the event, depending on physics cases. An example application is the search for $pp \to ZH$ production in which Z and H decay into two neutrinos and two b-jets, respectively. Figure 7 shows the smallest azimuthal angular distance between $E_{\mathrm{T}}^{\mathrm{miss}}$ and jet trigger objects, which demonstrates a significant improvement of the signal discrimination from minimum bias background events.

6. Conclusion

New architectures of the ATLAS LAr trigger readout and L1Calo processing system have been developed toward the Run-3 data taking period scheduled to start in 2019, which enables more refined processing of EM calorimeter information and provides various new features of the calorimeter trigger. By adopting them, ATLAS can retain a good trigger performance even in severe pile-up conditions and also improve the physics coverage by complementing inclusive trigger selection algorithms with more exclusive ones.

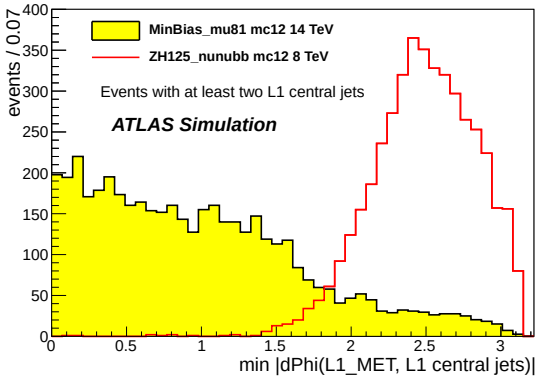

Figure 7: The smallest azimuthal angular distance between $E_{\mathrm{T}}^{\mathrm{miss}}$ and jet trigger objects for $ZH \to \nu\bar{\nu}b\bar{b}$ and minimum bias events [3].

Acknowledgments

This work was supported by JSPS Grant-in-Aid for Young Scientists (A) 26707010 and Program for Advancing Strategic International Networks to Accelerate the Circulation of Talented Researchers R2602.

References

[1] ATLAS Collaboration, 2008 JINST 3 S08003.
[2] ATLAS Collaboration, CERN-LHCC-2013-017, `http://cds.cern.ch/record/1602230`.
[3] ATLAS Collaboration, CERN-LHCC-2013-018, `http://cds.cern.ch/record/1602235`.
[4] ATLAS Collaboration, Eur. Phys. J. **C70** 823 (2010).